Taylor & Francis
Taylor & Francis Group

Quantitative InfraRed Thermography Journal

ISSN: 1768-6733 (Print) 2116-7176 (Online) Journal homepage: https://www.tandfonline.com/loi/tqrt20

Lock-in thermography for analyzing solar cells and failure analysis in other electronic components

Otwin Breitenstein & Steffen Sturm

To cite this article: Otwin Breitenstein & Steffen Sturm (2019) Lock-in thermography for analyzing solar cells and failure analysis in other electronic components, Quantitative InfraRed Thermography Journal, 16:3-4, 203-217, DOI: 10.1080/17686733.2018.1563349

To link to this article: https://doi.org/10.1080/17686733.2018.1563349

Published online: 22 Feb 2019.

QUANTITATIVE INFRARED THERMOGRAPHY JOURNAL
2019, VOL. 16, NOS. 3–4, 203–217
https://doi.org/10.1080/17686733.2018.1563349

Taylor & Francis
Taylor & Francis Group

REVIEW ARTICLE

OPEN ACCESS Check for updates

Lock-in thermography for analyzing solar cells and failure analysis in other electronic components

Otwin Breitenstein[a] and Steffen Sturm[b]

[a]Max Planck Institute of Microstructure Physics, Halle, Germany; [b]InfraTec GmbH, Dresden, Germany

ABSTRACT

Lock-in thermography (LIT) is a dynamic variant of infrared thermography, where local heat sources are periodically pulsed and amplitude and phase images of the surface temperature modulation are obtained. If used in electronic device testing, this method enables the localization of very weak local heat sources below the surface. This contribution reviews the basics and application of LIT for local efficiency analysis of solar cells and for failure analysis in other electronic components like bare and encapsulated integrated circuits. In both application fields LIT has established as a reliable and easy-to-use standard method for failure analysis.

ARTICLE HISTORY
Received 29 October 2018
Accepted 21 December 2018

KEYWORDS
Lock-in thermography; electronic devices; failure analysis

1. Introduction

Lock-in thermography (abbreviated LIT or LT), which is the phase-locked detection of local periodic surface temperature modulations in a device by an infrared (IR) camera, was proposed in 1985 by Beaudoin et al. [1] and used for detecting a thin plastic film on a rubber sheet. In 1988 lock-in thermography was used for the first time with on-line data evaluation for investigating micro-cracks in an electrically heated Cu foil on polyimide substrate [2]. Already here local heat sources in an electronic device have been imaged. Later on LIT became more popular for non-destructive testing (NDT) of constructional materials like airplane components, since photo-thermal investigations allow to 'look below the surface' of such components [3,4]. Other applications of LIT in NDT were thermo-elastic [5] and ultrasonic lock-in thermography (ULT [4]). Only after 2000, LIT was applied systematically again for failure analysis in electronic components like solar cells and integrated circuits (ICs) [6]. While in NDT certain inhomogeneities of the investigated material are in focus (e.g. delaminations, anisotropic thermal properties, missing weld connections, or hidden cavities), the main goal of electronic device testing (EDT) is the detection of local heat sources in a thermally homogeneous device operating or under specific electronic test conditions. This is explained in Figure 1 illustrating the operation principles of NDT (a, taken from [4]) and of EDT (b). For NDT the case of photothermal investigation is shown and for EDT the case of dark lock-in thermography (DLIT) using a pulsed bias (operation voltage) of the device.

The success of LIT for EDT relies on the fact that all these devices generate heat in operation, hence they contain local heat sources. If there are certain faults in these

CONTACT Otwin Breitenstein breiten@mpi-halle.mpg.de MPI Halle, Weinberg 2, Halle 06120, Germany

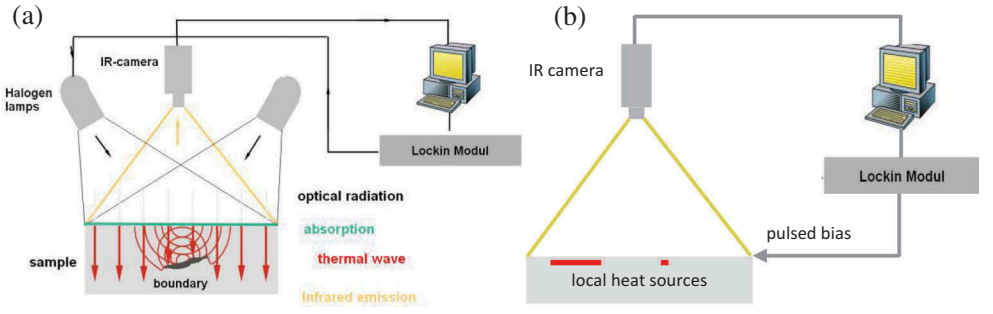

Figure 1. Functional scheme of (a) non-destructive testing [4] and (b) electronic device testing.

devices, these faults usually lead to a change in the distribution or in the generation of new local heat sources. Therefore, already before the advent of LIT, conventional (steady-state) thermography has been a standard tool for characterizing electronic components. However, since the noise limit of conventional thermography is in the range of 20. 100 mK, this technique allowed only the detection of relatively strong local heat sources. Moreover, due to the lateral heat conduction in solid devices, local heat sources generally appear blurred in steady-state thermography. These two limitations are strongly improved if LIT is applied instead of conventional thermography in EDT. Due to the averaging nature of LIT, the detection sensitivity lowers to 100 µK temperature modulation amplitude and below, and, due to its dynamic nature, lateral heat conduction is strongly suppressed. Moreover, LIT provides easy means of local emissivity correction, in particular for microscopic IC investigations.

In this contribution the application of LIT to EDT will be reviewed. Currently the two main application fields are the shunt imaging and local efficiency analysis of solar cells and failure analysis on other electronic devices. These are in particular microscopic LIT investigations in ICs and more macroscopic investigation of faults, like internal shorts in encapsulated ICs, printed circuit boards (PCBs), and other electronic components.

2. Basics of lock-in thermography for electronic device testing

Though commercial lLIT systems, like the PV-LIT system of InfraTec (www.infratec-infrared.com), can be used both for NDT and EDT, there are some particularities for LIT application to EDT. For example, LIT for EDT uses as a rule synchronous correlation, hence a well-defined number of camera frames is evaluated in each lock-in cycle [6]. For NDT the IR camera cannot always be synchronized to the lock-in process, but for EDT the pulse trigger can easily be derived from the camera frame trigger. While in NDT often sinusoidal modulation of the heat sources is applied, in EDT usually square pulse modulation is used, since here we are interested to operate an electronic component at a well-defined supply voltage. The evaluation of only the basic harmonic of the temperature- (*T*-) modulation is ensured by applying sin/-cos correlation [6]. In EDT the -cos correlation is used instead of the usual +cos correlation since only the −90° image is positive, see Figure 2. There are several possibilities to perform a LIT experiment on an electronic device. In simplest case a well-defined supply voltage (bias) of this

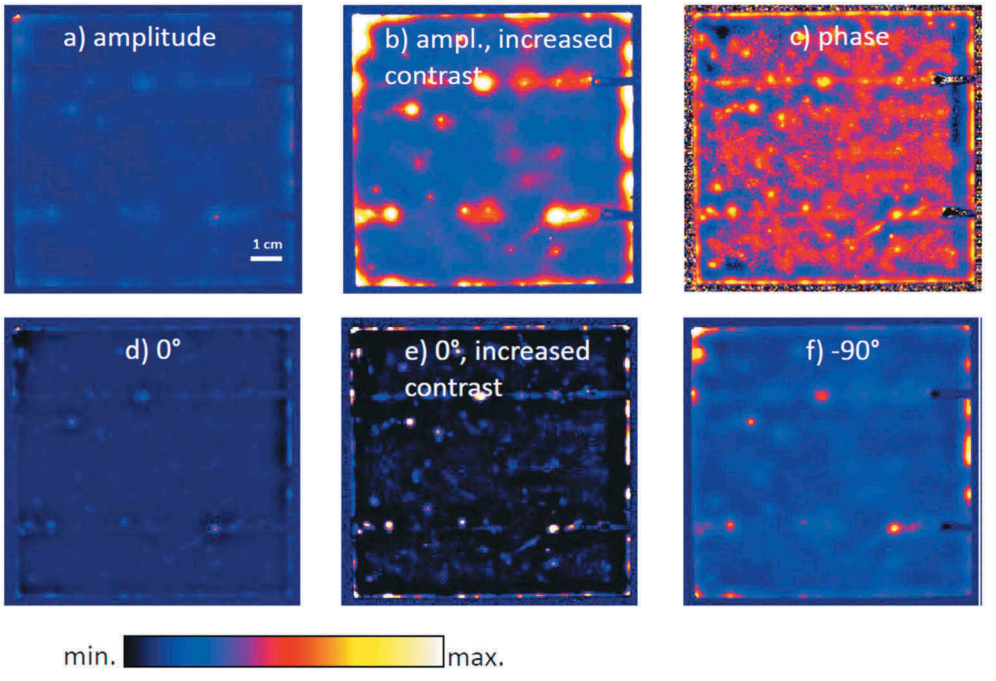

Figure 2. Different ways to display LIT results of a solar cell [6], see text.

device is periodically switched on and off in the dark (dark lock-in thermography, DLIT). All images shown in this work were measured in this way, hence electric excitation was used. The lock-in frequency used was always 10 Hz if not otherwise mentioned. Some devices lose their operation status if they are completely switched off. Then their operation voltage is modulated between two different biases. For integrated circuits like microprocessors it is also possible to keep the operation voltage constant and to modulate the internal operation periodically by using a programmable IC testing station. For solar cells also pulsed or steady-state light can be irradiated, instead of or in addition to bias modulation. These experiments are called illuminated LIT (ILIT) [6].

Another difference to LIT for NDT is that for EDT not only the amplitude and phase images are evaluated, which is standard in NDT, but also the primary in-phase (0°) and out-of -phase (–90°) images are of interest. Figure 2 shows all these images resulting from one LIT measurement of a multicrystalline silicon solar cell. If the amplitude image is scaled to the maximum signal, as in image (a), only the strongest local heat source in the upper left corner becomes clearly visible. If the same data are displayed with increased contrast (b), many other local heat sources (in particular in the edge region) and also the homogeneous heating in the whole area become visible. The phase image (c) represents the time delay between the power modulation and the resulting temperature modulation. For isolated point-like heat sources this phase signal is independent of the power of the source. Therefore in the phase image (c) local heat sources of different magnitude appear with nearly the same brightness. This may be called a 'dynamic compression' feature of the phase signal in EDT. Another property of the phase signal, which is also known from NDT, is its independence of the local IR emissivity. The in-phase (0°) signal in Figure 2(d,e) shows the

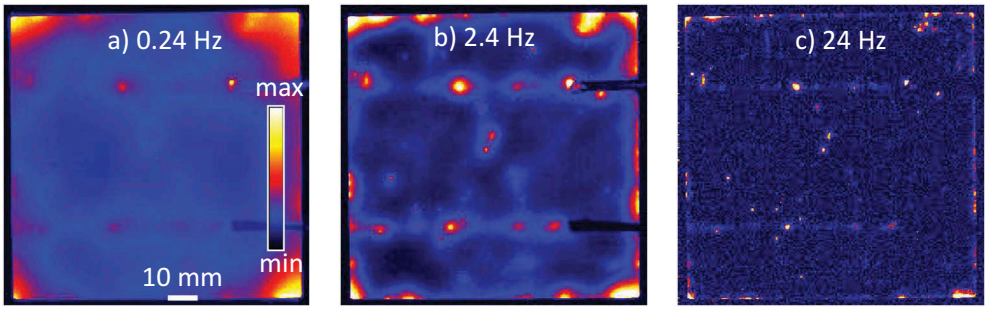

Figure 3. Amplitude images of a solar cell taken at various lock-in frequencies.

best spatial resolution of all LIT signals and is therefore most appropriate for imaging point-like heat sources. This is best visible in image (e) showing increased contrast. Outside of these local heat sources, however, the 0° signal shows an overshoot into the negative. Homogeneous heat sources remain completely invisible in the 0° signal of a solar cell, since for them the temperature modulation occurs at a phase of −90° [6]. In EDT the −90° signal (f) is always displayed instead of the +90° signal, since the latter is always negative because the *T* modulation is more or less delayed to the power modulation (delay means negative phase). This −90° signal shows the worst spatial resolution of all LIT images. Its spatial resolution is in the order of the thermal diffusion length, which is about 2 mm for a silicon device pulsed at 10 Hz and reduces with $1/\sqrt{f_{lock\text{-}in}}$ [6]. However, the −90° signal displays both local and homogeneous heat sources and is therefore best appropriate for displaying the local dissipated power density, see Section 3.2. If integrated circuits (ICs) are investigated (see Section 4), except of the LIT images always a topography image must be taken, which is just a single IR image of the unpowered device. Then there must be the option to superimpose the topography and the LIT image, since only then a local fault can be attributed to a certain position in the layout of the IC. The PV-LIT system of InfraTec, which is particularly appropriate for EDT, implies all these options.

One of the most important parameters of LIT is the lock-in frequency. It governs the thermal diffusion length, which determines the effective spatial resolution of LIT images, see above. On the other hand, the lock-in frequency determines the obtained signal-to-noise ratio (SNR). The higher the lock-in-frequency, the poorer becomes the SNR, since the temperature modulation amplitude becomes smaller. This is demonstrated in Figure 3 where the influence of the lock-in frequency on the amplitude image of a solar cell is shown. The increasing spatial resolution for increasing lock-in frequency is obvious. On the other hand, in Figure 3(c) the amplitude noise becomes already visible.

3. Lock-in thermography for solar cell analysis

3.1. LIT for shunt imaging

LIT was first applied to solar cells for imaging so-called shunts. Figure 4 shows schematically two dark (top) and two illuminated current-voltage (*I-V*) characteristics (bottom, red) of solar cells, with and without shunts, all under forward bias. In the dark, positive voltage (forward bias) leads to positive currents, hence the cell dissipates power. The

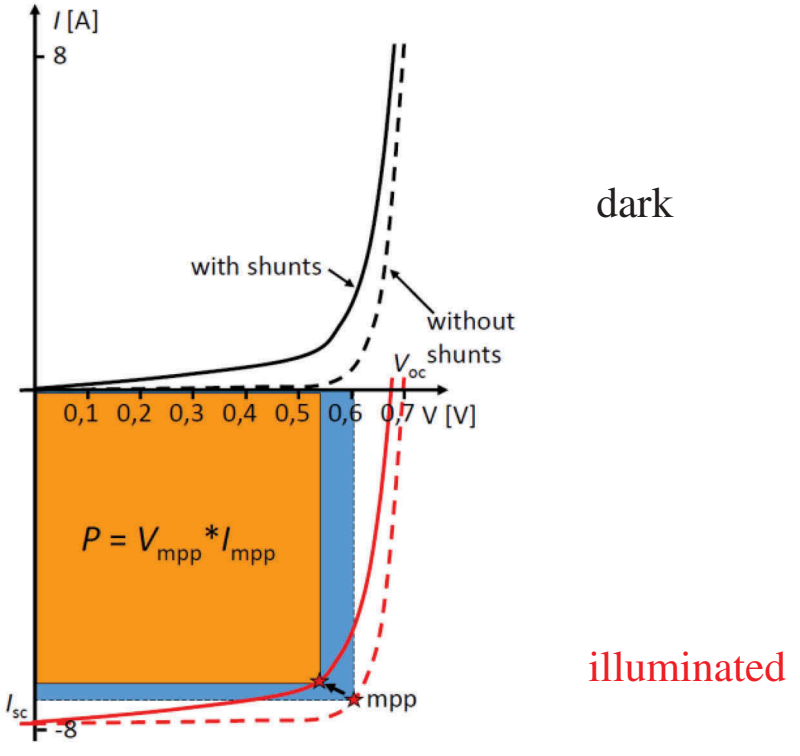

Figure 4. Dark I-V characteristics (top) and illuminated characteristics (bottom) of a solar cell with and without shunts, see text.

dark characteristic is essentially exponential, hence for low biases the dark current is negligibly small and then it strongly increases with increasing forward bias. It is often assumed that the dark current flows homogeneously in solar cells, but this is as a rule not true. Nearly all solar cells contain local positions showing a strongly increased dark current. These positions are traditionally called 'shunts'. The bright spots visible in Figures 2 and 3 are typical shunts. These shunts may show a linear (ohmic) or a diode-like characteristic, but they generally tend to increase the dark forward current as shown in Figure 4 at the top. If a solar cell is illuminated, in addition to the voltage-dependent dark current the photocurrent flows. This photocurrent is by nature a reverse (negative) current and it is essentially voltage-independent. Therefore the illuminated characteristic of a solar cell can be described in good approximation as the dark characteristic shifted to negative current values by a constant current, which is the so-called short circuit current I_{sc}. This transformation is called the superposition principle, since the positive dark current and the negative photocurrent linearly superimpose. Under illumination, the current may flow out of the cell, hence it is negative for positive biases and the cell produces electric power. If no current is extracted, the open circuit voltage V_{oc} establishes. The working point, where the maximum possible power P can be extracted, is the so-called maximum power point (mpp). At this maximum power point the product of generated current I_{mpp} and voltage V_{mpp} is maximum, which is symbolized in Figure 4 by the rectangular areas. If there are shunts in the cell, both the dark and the illuminated

characteristic change, as visible in Figure 4. Then I_{mpp} and V_{mpp} reduce, leading to a reduced generated power P and thus to a reduced energy conversion efficiency of the cell. Therefore all shunts are detrimental for obtaining a good cell efficiency and must be detected and, if possible, avoided. Shunts may be material-induced, e.g. if the cells consist of multicrystalline instead of monocrystalline silicon material, or they can be process-induced, e.g. by scratches during transportation of the wafers in manufacturing. LIT performed in the dark (DLIT) is the technique of choice for shunt imaging in solar cells. Once the positions of shunts have been found, their physical nature can be investigated by applying both LIT and other physical and microscopic investigations.

In principle, local shunts could also be made visible in solar cells by applying standard (steady-state) thermography. Indeed, standard thermography is a proven tool for characterizing large solar modules [7]. However, in single solar cells only very strong shunts could be detected, since the sensitivity even of the best modern thermocameras is only in the order of 20 mK. This is enough for detecting shunts under higher reverse bias of, say, −10 V, but not for detecting shunts under forward bias, which is most interesting since under operation the cell is forward biased by about 0.55 V, see Figure 4. Moreover, under steady-state condition the surface temperature profile around local shunts appears very blurred, since the heat tends to diffuse away laterally from the heat sources. Note that silicon is a quite good heat conductor. For LIT, on the other hand, the image noise is greatly reduced by averaging over many lock-in periods, and lateral heat diffusion is suppressed by the dynamic nature of the technique. Note that heat flow in a body takes time. Therefore, LIT can detect orders of magnitude more and weaker local shunts than steady-state thermography can do, which is illustrated in Figure 5. Here in (a) a standard (d.c.) thermogram of a solar cell at a relatively high forward bias and current is shown. We see that indeed the heat generation seems to be inhomogeneous and has a maximum in the middle of the lower contact stripe (busbar). The DLIT image (b) taken under the same biasing conditions shows this site and a large number of local shunts well-separated from each other. We see that, for the lock-in frequency of 10 Hz used here, the shunts show a T-modulation amplitude in the low mK range, which is typical. For LIT lateral heat conduction leads only to certain halos around the local shunts. The spatial extension of these halos can be reduced by increasing the lock-in frequency, but this goes on cost of the DLIT signal height, hence it would degrade the signal-to-noise ratio. Hence, the choice of the lock-in frequency represents

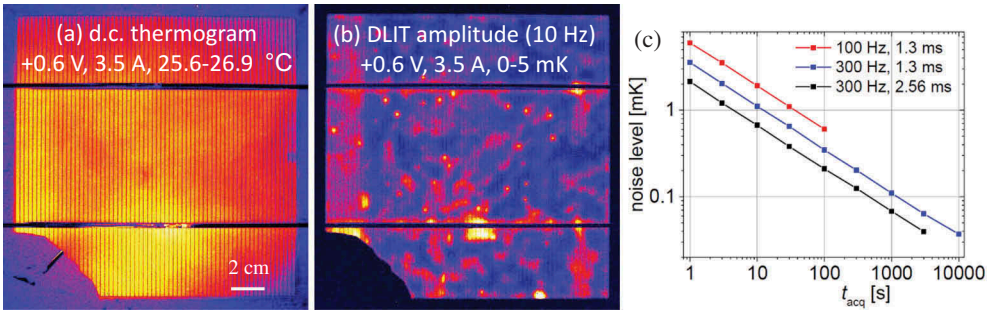

Figure 5. (a) Steady-state (d.c.) thermogram and (b) dark lock-in thermography image of a solar cell under identic conditions, (c) measured amplitude noise levels of the InfraTec PV-LIT system.

a compromise between high detection sensitivity (low frequency) and high spatial resolution (high frequency). Figure 5(c) shows the measured amplitude noise signal (objective cap closed) of the PV-LIT system of InfraTec (640 × 512 pixel InSb detector, 512 × 512 pixels used) as a function of acquisition time for different camera frame rates and frame integration times. The higher the frame rate and the frame integration time, the lower is the noise level [6]. At t_{acq} = 1000 s, which is below 17 minutes, a noise level below 100 µK may be obtained.

The amount and the polarity of the pulsed bias applied to a solar cell in a DLIT experiment allow to draw conclusions about the physical nature of the detected shunts. This is demonstrated in Figure 6 showing DLIT images of a solar cell under 500 mV forward bias (a), −500 mV reverse bias (b), and −12 V reverse bias (c). Only the shunts visible under forward and low reverse bias with the same brightness are ohmic shunts showing a linear *I-V* characteristic. All shunts appearing only under forward bias show a non-linear (diode-like) *I-V* characteristic. At higher reverse bias (c) local breakdown sites become active, which is a different conduction mechanism than that under low forward and reverse bias.

3.2. Quantitative evaluation of LIT images of solar cells

The silicon solar cells to be investigated by LIT consist of a 180 µm thick sheet of silicon. At a typical lock-in frequency of 10 Hz the thermal diffusion length is about 2 mm, hence this device can be considered as thermally thin [6]. This silicon material is thermally homogeneous. The metallic gridlines, which are used for feeding away the current, are only 10. 20 µm thick. Hence they do not influence the thermal properties significantly and can be penetrated easily by the thermal waves. However, their IR emissivity is significantly lower than that of the bare cell surface. Therefore, if bare solar cells are imaged by LIT, the gridlines always appear dark as could already be seen in Figure 5(b). It was mentioned in Section 2 that the −90° signal is proportional to the locally dissipated power density. This only holds correct if the emissivity is homogeneous. The usual possibility to homogenize the emissivity is to cover it by black paint. For solar cells, which have to convert light into electric energy, this is usually not wanted.

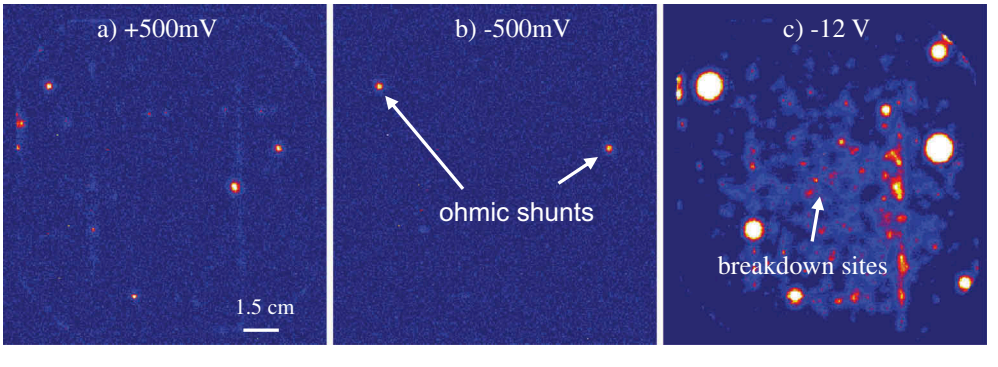

Figure 6. (a) Forward bias and (b) low reverse bias LIT amplitude image showing shunts with linear (ohmic) and non-linear characteristic, (c) high reverse bias amplitude image showing in addition breakdown sites.

One other possibility is here to suck-on by vacuum a 20 µm thin black plastic foil, as it is used for packaging purposes [6]. However, for frequencies of 10 Hz and above this foil leads already to a significant damping of the thermal waves. Here software-controlled local emissivity correction can be applied. The PV-LIT system of InfraTec provides the possibility to capture thermograms of the un-powered device at two temperatures and to calculate an image of the local emissivity, which is used to correct the LIT images. Reflected light needs not to be corrected in LIT since it is not modulated. In Figure 7 two LIT amplitude images are compared, one taken without and one with local emissivity correction. The emissivity-corrected image is best appropriate for quantitative evaluation, but also by using the un-corrected images the resulting quantitative error is only weak since the gridlines occupy only a small fraction of the area.

It was mentioned in Section 2 that the 0° image shows a sharp maximum in the position of local shunts and becomes negative in greater distance to the shunts, its average over the area is zero. The LIT amplitude image, which is always positive, is the vectorial sum of the 0° and the −90° images. For several shunts closely located to each other the horizontally running thermal waves superimpose. Then only the vectorial components (0° and −90° images) superimpose linearly, but not the amplitude signals, since the amplitude is a non-linear combination of the vectorial components. Therefore the amplitude signal is less appropriate for quantitative evaluation, since it would overestimate the signal close to local shunts. As already mentioned in Section 2, the local −90° signal $S^{-90^\circ}(x,y)$ is best appropriate for quantitative evaluation, since, in the limit of its low spatial resolution, it is strictly proportional to the locally dissipated heat. Note that each LIT system shows a systematic phase error due to the processing times needed for the digital signal processing. For performing quantitative LIT evaluation this phase error should to be corrected. This can be done by zeroing the averaged 0° signal; the PV-LIT system of InfraTec contains an automatic option for this. The proportionality factor between the −90° signal and the local power density is found by evaluating the average of the −90° signal over the whole solar cell $<S^{-90^\circ}>$, which must be proportional to the whole dissipated power (product of measured voltage V and current I during the

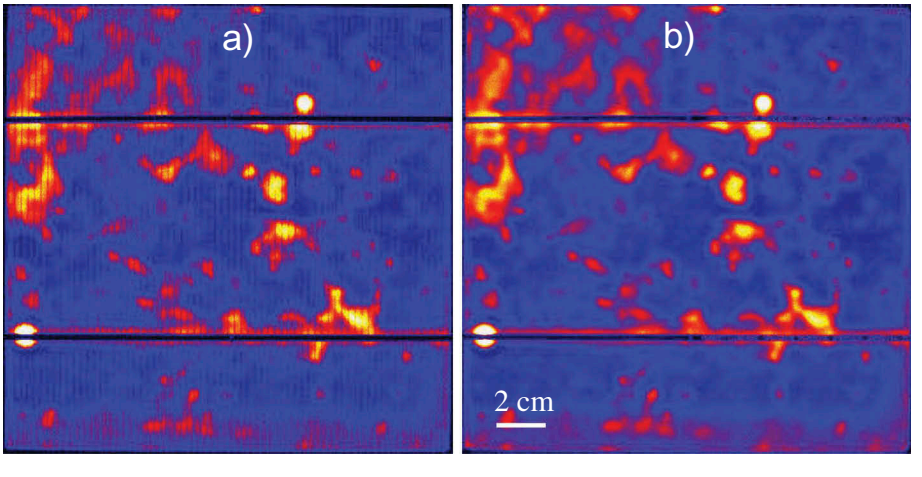

Figure 7. LIT amplitude images of a bare silicon solar cell (a) without and (b) with local emissivity correction.

excitation pulses). This leads to the following simple formula for converting −90° LIT images to images of the dissipated power density p (A = cell area):

$$p(x,y) = \frac{S^{-90^\circ}(x,y)V\ I}{A\ \langle S^{-90^\circ}\rangle} \tag{1}$$

Note that this formula is 'self-calibrating', hence it needs neither the thermal parameters of the object nor any sensitivity parameter of the IR camera. Based on this formula the software program 'Local I-V 2' for evaluating LIT images has been developed for performing the so-called 'Local I-V' method, which is available [8]. This software evaluates up to four −90° DLIT images, three measured at different forward biases and one measured under weak reverse bias, where no breakdown processes are expected. As its name says, the 'Local I-V' method is used for non-destructively (thermally) measuring local I-V characteristics of solar cells. This method and its application to typical solar cells is described in detail in [9,10], therefore only its basic principles and some selected results will be reported here. The software first converts all entered LIT images into local power density images by using (1). Then it converts these images into images of the local current density and the local diode voltage by considering the effective local series resistance R_s(x,y). This series resistance may be assumed to be homogeneous, an R_s image may be imported e.g. from luminescence measurements [11], or a luminescence-measured local diode voltage image is imported and evaluated together with LIT results as described in [12]. The local dark current densities are then fitted for each image pixel separately to the so-called two-diode model, which is the standard model for describing dark and illuminated characteristics of solar cells [6,9]. Once the parameters of the two-diode model for each pixel are known, the software calculates local dark and illuminated characteristics for each pixel by using the superposition principle described in Section 2.

Figure 8 shows a selection of *I-V* characteristics measured thermally by 'Local I-V' in four different positions of a solar cell. There are three physically different dark current contributions in a solar cell, which are the diffusion current J_{diff}, which is the nominal diode current, the depletion region recombination current J_{rec} flowing only in certain shunt positions, and the ohmic shunt current J_{shunt}, which can be due to local material defects or technological faults. The diffusion current shows the fastest increasing exponential characteristic, the recombination current a weaker increasing exponential characteristic, and ohmic shunts show a linear characteristic. By taking into account these different voltage dependencies, these three components are separated from each other in 'Local I-V'. The images in Figure 8 show the dominating components of the dark characteristics (J_{diff}, J_{rec}, and J_{shunt}), the sum dark characteristics (J_{sum}), and the resulting illuminated characteristics (J_{illum}) in 4 positions of a cell. The black dots are the points where the current densities were measured by DLIT under forward bias.

We see that these characteristics differ significantly from each other, pointing to the different physical origins of their dominating components. The position 'J_{diff} shunt' is a local maximum of the diffusion current, 'J_{rec} shunt' is a local maximum of the recombination current, and 'ohmic shunt' is a shunt with a linear characteristic. Based on these local characteristics, 'Local I-V' calculates images of important solar cell parameters, like the open circuit voltage V_{oc}, the fill factor (a measure of the rectangular shape of the illuminated characteristic), or the conversion efficiency [10]. Such investigations are very helpful in the

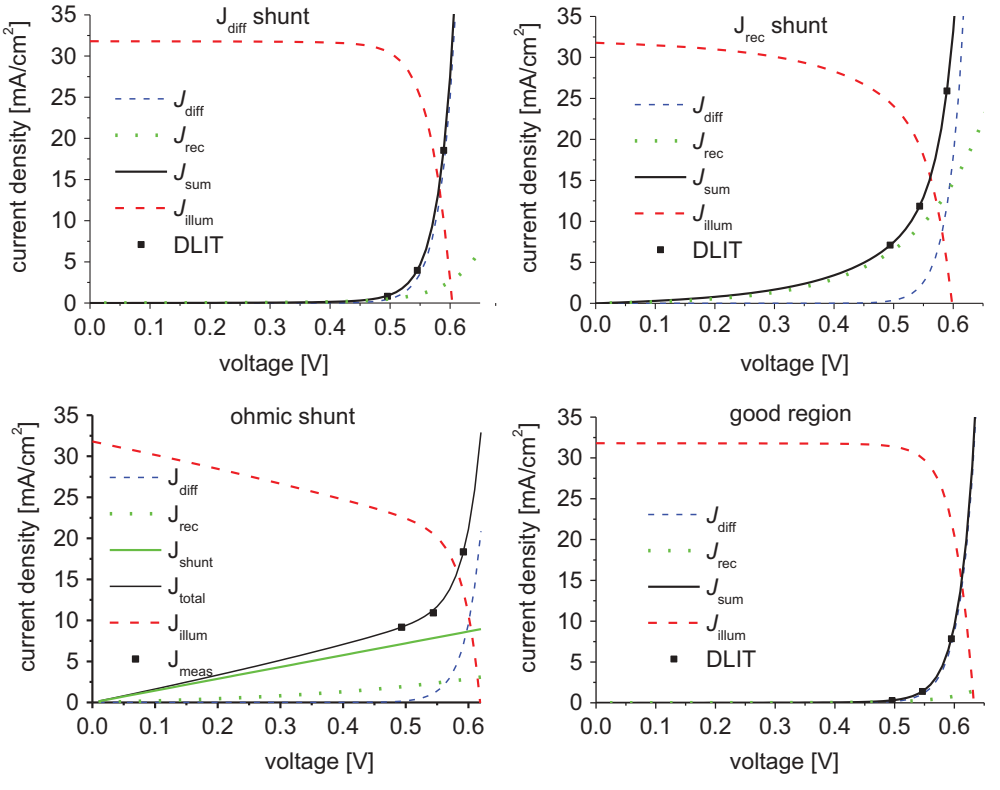

Figure 8. Thermally measured dark and illuminated local I-V characteristics of different positions in a solar cell (J_{diff} shunt, J_{rec} shunt, ohmic shunt, and in a good region, see text).

process of looking for physical origins of poor efficiency parameters and are an example par excellence for quantitative IR thermography (QIRT).

4. Lock-in thermography for bare and encapsulated ICs

Since its introduction to integrated circuit (IC) failure analysis (FA) in 2000 [13], LIT has become a standard method also in this field. The success of LIT for IC FA relies on the fact that many faults in ICs, like internal shorts, latch-ups, faulty transistors or diodes, or other leakage currents, generate local heat. For these investigations generally mid-wave IR cameras are used, for which, even with the best available microscope objective lenses, the diffraction-limited spatial resolution is in the order of 5 µm. This resolution can be reduced down to about 1.5 µm by applying a solid immersion lens (SIL) [14]. Such an immersion lens is basically a hemispherical piece of silicon, positioned with its flat side on the flat surface of the IC. If there are local heat sources directly below the surface of the IC (the active layer of an IC is always directly below the surface), the space above the heat source is then filled by silicon instead of air. Since the refraction index of silicon is 3.5, the wavelength of the contributing thermal radiation (for an InSb camera about 5 µm in air) is reduced by this factor, leading to a correspondingly increased diffraction-limited spatial resolution. Optically, the SIL acts for the following microscope objective lens as a magnifying glass with a magnification factor of 3.5. Figure 9 shows such a SIL

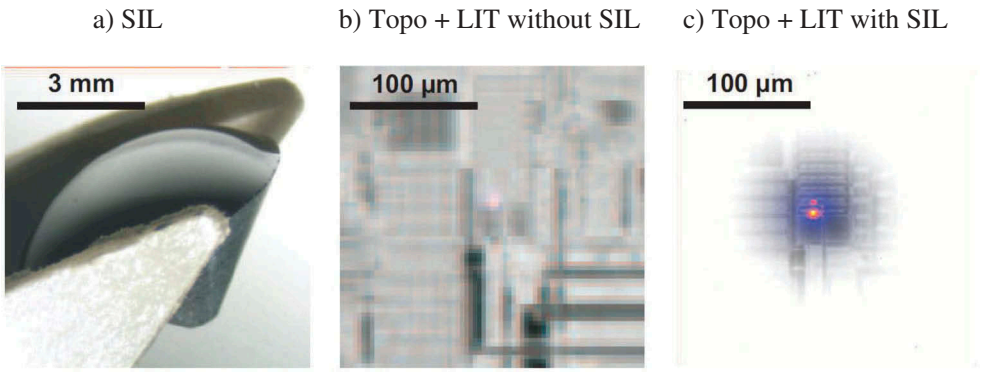

Figure 9. (a) Solid immersion lens (SIL), (b) region in an IC imaged without SIL (amplitude + topography signal), the same imaged with SIL [15].

and LIT images (amplitude images superimposed to the topography images) of a local heat source in IC images without (b) and with SIL (c) [15]. The increased brightness in (c) in the edge region stems from the topography image. Here the inclined surface in this region reflects thermal radiation from the environment into the objective lens, whereas in the centre of the image the Narcissus effect dominates.

Even with the use of a SIL the structural dimensions of present ICs are with <0.1 µm still below the spatial resolution of LIT. Nevertheless LIT is very successful for at least a first coarse localization of faults due to its extreme sensitivity and easy applicability. Once a fault is localized by LIT to an accuracy of a few µm, its detailed position may be revealed later on e.g. by light emission microscopy, electron beam methods, laser-based methods, or electric nano-probing methods [16].

Figure 10 shows a topography image (a) and a LIT amplitude image (b) of an intact IC with the supply voltage pulsed. The bright spots in (b) are due to the normal operation of this IC. Figure 10(c) shows the LIT amplitude image of a defect IC of the same type. Here two additional bright spots are visible, which indicate the locations of the faults being responsible for the defect in this IC.

A particular problem for LIT on bare ICs is the inhomogeneous IR emissivity, which is much lower in metallized than in non-metallized regions. If a magnifying microscope

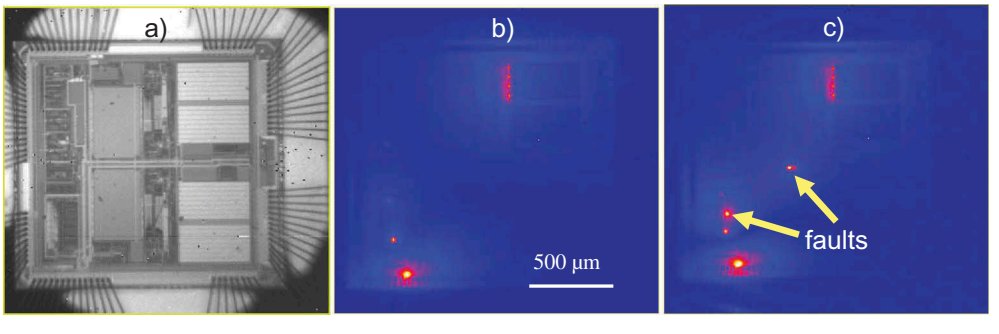

Figure 10. (a) Topography image and (b) LIT amplitude image of an intact IC, (c) LIT amplitude image of a faulty IC. Lock-in frequency: 20 Hz. The arrows point to the fault locations.

objective is used, the image field is smaller than the detector. Then the whole image field is within the black spot of the 'Narcissus effect', hence the metallization appears in topography dark, and not metallized regions appear bright. If the image 'wiggles' e.g. due to vibrations caused by the Stirling cooler of the IR camera, on each bright-dark-edge a strong intensity modulation appears, which is interpreted by the lock-in correlation procedure wrongly as a LIT signal. These artifacts can be minimized by choosing a lock-in frequency, which is sufficiently apart from the vibration frequency and its harmonics. An off-line correction of these artifacts is not possible. For avoiding image wiggling, a mechanically strong connection must be established between camera (the objective) and the imaged object. InfraTec provides a very stable camera support with a x-y table for performing LIT for IC analysis.

Even if the image does not wiggle, local emissivity correction as described in Section 3.2 is hardly applicable in microscopic regions, since it is hard to avoid microscopic lateral image movement if the device temperature is changed. If the images at the two temperatures are not exactly in the same position, the obtained emissivity image shows strong artifacts on edges of the metallization. Here the display of the 0°/-90° signal is very helpful, as it is demonstrated in Figure 11, see [17]. This figure shows various representations of LIT results of a region in an IC. In the topography image (a) we see the strong emissivity contrast, all regions appearing dark are metallized regions. The 0° signal (b) shows the best spatial resolution, but it is also modulated by the emissivity contrast. The phase signal (d) does not show any emissivity contrast, but it shows a low spatial resolution and, due to the dynamic compression feature mentioned in Section 2, it is not proportional to the dissipated power density. The −90° signal (c) shows only a weak maximum in the position of the dominant 0° signal. This is due to the inherently low spatial resolution of this signal of about 2 mm here, which was mentioned already in Section 2. Hence the −90° *T*-modulation is nearly homogeneous in this small region, but the −90° IR image is modulated by the local emissivity. Indeed, the −90° signal (c) looks similar to the topography signal (a), but in

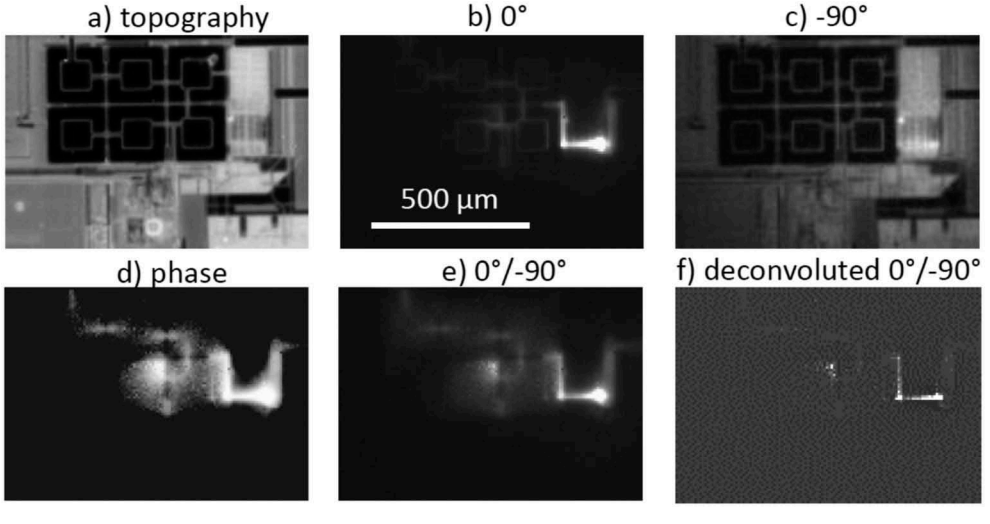

Figure 11. (a) Topography image, (b) 0° image, (c) −90° image, (d) phase image, (e) 0°/−90° image, and (f) spatially deconvoluted 0°/−90° image of a region in a bare IC.

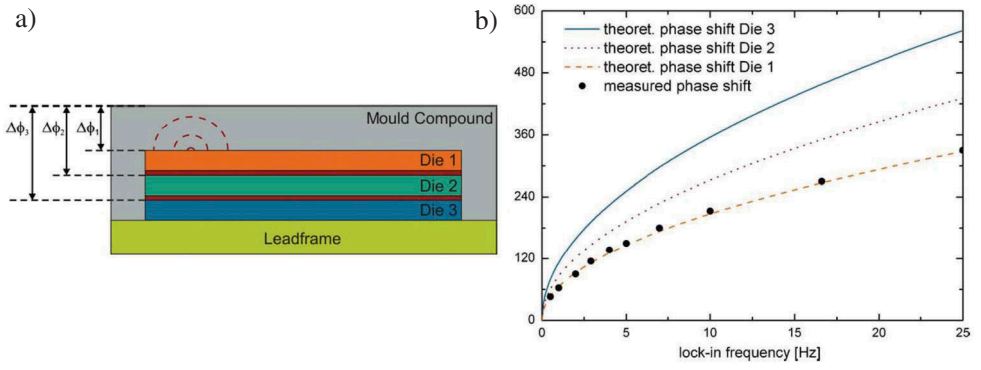

Figure 12. (a) Cross section through a stacked IC, (b) simulated (theoretical) phase shift (in degrees) for a defect lying in different dies of the IC and measured phase shift values for different lock-in frequencies.

contrast to this it shows a well-defined zero signal level. Therefore, in micro regions where the thermal diffusion length exceeds the image size, the −90° signal can be used as a measure of the local emissivity. Then the 0°/−90° signal (e) is an 'emissivity-corrected 0° signal'. This signal can even be mathematically deconvoluted for improving its spatial resolution (f), which, however, increases the noise level [17].

A more recent development is 3D Analysis of encapsulated stacked ICs [18]. In particular for memory devices it is usual to glue several thin chips (called 'dies', thinned down to about 20 µm thickness) on top of each other for increasing the packing density. Then, if the whole device should show a heat-producing fault, it is interesting to know in which of the stacked dies the fault is located. This can be measured by measuring the frequency-dependence of the phase of the temperature modulation at the surface of the mould compound used for encapsulating the IC. If the thermal wave travels vertically from the fault position to the surface of the device, at the junction from each die to die a phase shift occurs due to the heat capacity of the die and the heat resistance of the glue layer between the dies, some µm in thickness. In the top mould compound an additional phase shift occurs. This is illustrated in Figure 12(a). Hence, depending on in which die the fault is located, a different frequency-dependent phase of the temperature modulation at the surface is expected. This can be numerically modelled if the thermal properties and the dimensions of all layers are known. Figure 12(b) shows the result of such a measurement together with theoretical calculations of the phase shift for the fault located in different dies. In this case the fault was located in die no. 1 close to the surface, leading to the lowest amount of the phase shift.

5. Conclusions

Lock-in thermography (LIT) has established in the last 15 years as a standard method not only in non-destructive testing (NDT) but also in electronic device testing (EDT). For being useful in EDT, commercial LIT systems must fulfil certain special requirements, like special display options, the possibility to correct systematic phase errors, 4-wire connection to the sample with exact display of the applied voltage, local emissivity correction, and *T*-drift correction. Until now the main application fields of LIT in EDT are shunt imaging and local

efficiency analysis in solar cells and failure analysis in other electronic components like integrated circuits. However, LIT can be used to locate heat sources in any electronic device. If the devices are thermally homogeneous, the results can be evaluated in terms of measured power densities or depth of a heat-producing fault below the surface. For investigating solar cells, the 'Local I-V' method provides a powerful tool for performing a detailed quantitative local efficiency analysis. By this analysis local shunts, which are origins of degraded efficiency parameters of a cell, can be found and analysed and their influence on the solar cell efficiency can be determined. For investigating ICs, heat-producing faults can be localized up to an accuracy of 5 µm and up to 1.5 µm by using a solid immersion lens [6,14]. With the continuing trend of falling prices of IR cameras, it can be expected that the use of LIT in EDT will further increase.

Acknowledgments

The authors are grateful to F. Altmann and Ch. Schmidt (Fraunhofer IWM Halle), Jan Bauer and F. Frühauf (MPI Halle), and many other colleagues for experimental cooperation. Part of this work was supported by the German Federal Ministry for Economic Affairs and Energy in the "SolarLIFE" (0325763 D) and foregoing projects.

Disclosure statement

No potential conflict of interest was reported by the authors.

Funding

This work was supported by the German Federal Ministry for Economic Affairs and Energy in the 'SolarLIFE'; [0325763 D].

ORCID

Otwin Breitenstein http://orcid.org/0000-0002-4238-3973

References

[1] Beaudoin JL, Merienne E, Danjoux R, et al. Numerical system for infrared scanners and application to the subsurface control of materials by photothermal radiometry. Infrared Technol Appl SPIE. 1985;590:287.
[2] Kuo PK, Ahmed T, Jin H, et al. Phase-locked image acquisition in thermography. Proceedings of SPIE 1004, Automated Inspection and High Speed Vision Architectures II; 1988. p. 41.
[3] Krapez J-C, Gardette G, Balageas D Thermal ellipsometry in steady-state and by lock-in thermography. Application to anisotropic materials characterization. Proc. 3rd Int. Workshop on Advanced IR Techn. and Appl., Capri (It.); Sept 19–20; Fondazione G. Ronchi (Firenze); 1995. p. 219–237.
[4] Busse G. From photothermal radiometry to lock-in thermography methods. J Phys Conf Ser. 2010;214(1–7):012003.
[5] Harwood N. Cummings W.M. Thermoelastic stress analysis. Bristol: Adam Hilger; 1991.

[6] Breitenstein O, Warta W, Langenkamp M. Lock-in thermography – basics and use for evaluating electronic devices and materials. 2nd ed. Heidelberg: Springer; 2010.
[7] Buerhop C, Schlegel D, Niess M, et al. Reliability of IR imaging of PV plants under operating conditions. Solar Energy Mat Solar Cells. 2012;107:154–164.
[8] [cited 2018 Apr]. Available from: <www.maxplanckinnovation.de>
[9] Breitenstein O. Nondestructive local analysis of current-voltage characteristics of solar cells by lock-in thermograpphy. Solar Energy Mat Solar Cells. 2011;95:2933–2936.
[10] Breitenstein O. Local efficiency analysis of solar cells based on lock-in thermography. Solar Energy Mat Solar Cells. 2012;107:381–389.
[11] Trupke T, Pink E, Bardos RA, et al. Spatially resolved series resistance of silicon solar cells obtained from luminescence imaging. Appl Phys Lett. 2007;90(1.3):093506.
[12] Ramspeck K, Bothe K, Hinken D, et al. Recombination current and series resistance imaging of solar cells by combined luminescence and lock-in thermography. Appl Phys Lett. 2007;90 (1–3):153502.
[13] Breitenstein O, Langenkamp M, Altmann F, et al. Microscopic lock-in thermography investigation of leakage sites in integrated circuits. Rev Sci Instr. 2000;71(11):4155–4160.
[14] Breitenstein O, Altmann F, Riediger T, et al. Use of a solid immersion lens for thermal IR imaging. Proceedings of 32th Int. Symposium for Testing and Failure Analysis (ISTFA); Austin TX. 2006. pp. 382–388.
[15] Schmidt C [Ph.D. Thesis]. Halle: 2012.
[16] Ross RJ, ed. Microelectronics failure analysis: desk reference. 6th ed. Ohio: ASM Internationational; 2011.
[17] Breitenstein O. Lock-in IR thermography for functional testing of solar cells and electronic devices. Qirt J. 2004;1(2):151–172.
[18] Schmidt C, Altmann F, Breitenstein O. Application of lock-in thermography for failure analysis in integrated circuits using quantitative phase shift analysis. Mat Sci Eng B. 2012;177:1261–1267.